The effect of antibody protein dose on the uniformity of tumor distribution of radioantibodies: an autoradiographic study*

Rosalyn D. Blumenthal, Irwin Fand, Robert M. Sharkey, Otto C. Boerman, **Rina Kashi, and David M. Goldenberg**

Garden State Cancer Center and Center for Molecular Medicine and Immunology, Newark, NJ 07103, USA

Summary. The inaccessibility of radiolabeled antibody to poorly vascularized regions of solid tumors may reduce the therapeutic efficacy of these macromolecules. Theoretical mathematical models have predicted that increasing the protein dose administered would reduce the heterogeneity of radioantibody distribution. This investigation was undertaken to evaluate this hypothesis in experimental animal models. We have utilized the technique of macroautoradiography to demonstrate an increase in tumor penetration of the lower-affinity ^{125}I-labeled NP-4 or higher-affinity Immu-14 anti-carcinoembryonic antigen (anti-CEA) mAbs into small (60.25–0.4 g) and large (0.8–1.5 g) GW-39 and LS174T human colonic xenografts, grown subcutaneously in the nude mouse, when 400 µg unlabeled antibody is administered simultaneously with 10 µg (100 µCi) radioantibody. Further increases in protein to 800 µg result in a reduction in total tumor uptake of the antibody. These differences in mAb distribution could be visualized as early as 1 day after antibody injection. Improved mAb penetration was also achieved for the Mu-9 anti-CSAp (anti-mucin) antibody using 800 µg unlabeled antibody. An irrelevant antibody (AFP-7-31) was found to be homogeneously distributed 3 days after injection, even at a low protein dose. Attempts to improve mAb penetration by increasing the protein dose in the GS-2 colorectal tumor, a model that has low NP-4 accretion as a result physiological barriers separating antibody from antigen, were not successful. These results suggest that a more homogeneous distribution of radioantibody can be achieved by carefully selecting a dose of unlabeled antibody to coadminister. Work is currently in progress to determine the effect of improved tumor distribution of radioantibody on the therapeutic potential of a single dose of radioantibody.

Introduction

Radionuclides conjugated to antibodies have been evaluated in several experimental animal models [2, 8, 20, 49, 53] and clinical trials [9, 13] for their antitumor activity. Several investigators have demonstrated a heterogeneous distribution of antibody conjugates; penetration was restricted to a thin layer of tumor cells in the perivascular space [12, 38]. Although radioantibodies are potentially tumoricidal within several cell diameters (^{131}I energy deposited within a range of 0.99 mm and ^{90}Y effective in a range of 5.9 mm [16], large regions of tumor tissue would be expected to escape therapy as a result of being outside of the range of energy emission of the radionuclide. Overcoming this potential obstacle of nonuniform antibody distribution would be expected to enhance the therapeutic potential of these antibody conjugates.

Multicellular tumor spheroid systems have provided a useful in vitro model for studying the dynamic aspects of drug penetration [27, 34, 35, 44, 51]. Spheroids have been used to demonstrate that antibody fragments penetrate better than intact antibodies [44] and that an antibody cannot penetrate and bind with an antigen in well-polarized epithelial cells [39]. In vitro spheroid models are limited, however, in their usefulness; they ignore in vivo drug disposition [i.e., (a) passage of the drug from the site of administration to the site of pharmacological action, (b) role of plasma binding proteins, (c) transport from the vascular compartment to the target tissue, (d) effect of protein in the interstitial fluid, and (e) potential for metabolism]. Tumor xenografts have provided a useful in vivo model to address questions on antibody conjugate penetration into tumor tissue [7, 32, 36–38]. Immunohistology of a pancreatic tumor model has shown that intact IgG is
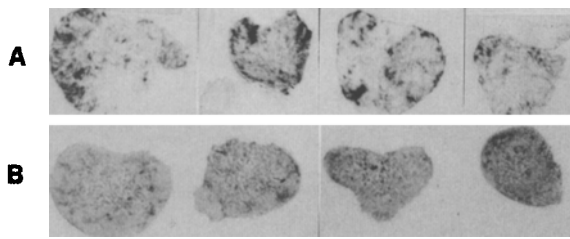
Fig. 1. Distribution of (**A**) specific antibody NP-4 anti carcinoembryonic antigen (CEA) IgG and (**B**) irrelevant antibody AFP-7-31-anti-AFP IgG in GW-39 tumors. Mice were sacrificed 3 days after injection of 100 μCi ^{125}I-labeled antibody

found in some highly vascularized areas but not in other areas, even though the epitope was present [7]. Pervez et al. have used autoradiography of LoVo colorectal xenografts to support the findings of the spheroid model; smaller-size F(ab')$_2$ fragments show better tumor penetration that intact antibody [37, 38]. However, Ong and Mattes have reported a homogeneous distribution of intact antibody in their solid tumor model, a human ovarian carcinoma [36]. Several differences exist between the model systems employed, which may account for the differences in the two sets of observations; e. g., size of tumor, distribution of antigen, time between antibody administration and evaluation, and method of evaluation. Further studies are therefore required to determine the specific limitations to the penetration of antibody conjugates in an in vivo model. Several mathematical models have been developed to determine the best approaches to improve uniform distribution of anticancer agents [17, 25, 46]. In summary, these models suggest that antibody penetration could be improved by (a) decreasing antibody affinity so that antigen-antibody binding is reduced and more free antibody is available to percolate through the tumor, (b) increasing the antibody (protein) dose to saturate all antigenic sites, and (c) using smaller molecules, i.e., antibody fragments with higher diffusion coefficients. However, the parameters considered in these theoretical papers have not been evaluated in established experimental animal models. In this paper, we provide the first assessment of protein dose in three colorectal xenograft models.

These studies have been done by macroautoradiography, a technique that has previously been used by us (a) to analyze antibody distribution and localization in hamsters bearing subcutaneous tumors [14], (b) to identify lung metastases that could not be detected by external imaging or direct tissue counting [40], and (c) to study the kinetics of radioantibody localization in relationship to regional cell viability [15].

Materials and methods

Experimental animal model. GW-39, a signet-ring colon carcinoma [19], LS174T, a moderately differentiated colon adenocarcinoma, and GS-2, a well-differentiated colon adenocarcinoma, were serially propagated as subcutaneous growths in 5- to 6-week-old female nu/nu mice (Harlan Sprague Dawley, Indianapolis, Ind.). Tumors were excised, minced with a scissors in 0.9% NaCl solution with gentamycin (100 μg/ml) and passed through a 40-mesh screen to obtain a 20% suspension. Subcu-

taneous tumors were initiated with 200 μl 20% tumor suspension. The size of the tumor was controlled by varying the amount of time between tumor implantation and injection of radioantibody. Studies were performed on tumors weighing 0.25–0.4 g and 0.8–1.5 g.

Antibody purification and labeling. All antibodies were purified from mouse ascites using protein A and ion-exchange chromatography over S-Sepharose (Pharmacia, Piscataway, N.J.). Low-affinity NP-4 anti carcinoembryonic antigen (CEA) mAb ($1 \times 10^8 M^{-1}$) and Mu-9 anti-CSAp have been described previously [18, 42]. Higher-affinity Immu-14 anti-CEA ($1 \times 10^9 M^{-1}$) and an irrelevant IgG of the same IgG1 isotype, AFP-7-31 were obtained from Immunomedics, Newark, N. J.

Intact antibody was radioiodinated with Na ^{125}I (Amersham) by the chloramine-T method [30]. Radioantibody was separated from free radioiodine by passage over a PD-10 column (Pharmacia) equilibrated with 0.04 M phosphate-buffered saline containing 1% human serum albumin. Each radioantibody preparation was evaluated for aggregation and for free iodine (<4%) by size exclusion by HPLC using a GF-250 (Dupont, Wilmington, Del.) column. Immunoreactivity of NP-4 and Immu-14 was confirmed by CEA-Affi-Gel-10 (77% for both antibodies) and for Mu-9 by CSAp-Affi-Gel-10 (Bio-Rad) immunoadsorption (84%). Low-protein doses contained 1 μg (100 μCi) labeled antibody. High-protein treatments were prepared by mixing 1 μg labeled material with a balance of unlabeled antibody (50–800 μg) prior to intraperitoneal injection.

Whole-tumor autoradiography. Following pentobarbital anesthesia and cervical dislocation, tumors were removed from mice, flash-frozen in hexane cooled to –70° C on solid CO_2 and embedded in carboxymethylcellulose. The block was then trimmed to the midline region in the sagittal plane and 50-μm sections were made with an LKB-PMV2250 cryomicrotome at –17° C at 250-μM intervals. The sections were mounted with transparent tape, freeze-dried for 3–4 days at –17° C, and then placed directly on Dupont MRF33 Blue film for about 13–15 days at –20° C. Rapid freezing and freeze-drying of cryosections ensures that no translocation of radioantibody occurs from the site of uptake. Exposure was made without the use of intensifying screens. Completed autoradiograms were processed using standard photographic methods. Sample autoradiograms were selected from the center of the tumor and comparisons were made between size-matched tumor samples.

Results

The technique of macroautoradiography can be used to demonstrate differences in the pattern of intratumor distribution of specific and irrelevant antibodies. Figure 1 illustrates the heterogeneous pattern of the specific antibody NP-4 anti-CEA in the GW-39 tumor and the more homogeneous pattern of the irrelevant antibody AFP-7-31 in size-matched samples of the same tumor taken 3 days after injection of the radioantibody. Regional NP-4 "hot-spots" can be seen more clearly in the upper panel of four tumors. The dense grains in these areas most likely represent sites where radioantibody has permeated tumor vessels and bound to available CEA. A similar antigenic barrier does not exist in these tumors for the anti-AFP antibody and, therefore, a greater degree of percolation of the irrelevant antibody occurs (lower panel).

It has been suggested that penetration of a specific radioantibody could be enhanced by increasing the protein dose to help saturate more of the antigenic sites and enhance the amount of free radioantibody available to distribute randomly through the tumor [17, 25]. Uptake studies with small tumors (0.2 g) suggest that around 100–200 μg unlabeled antibody is needed to saturate tumor

GW-39
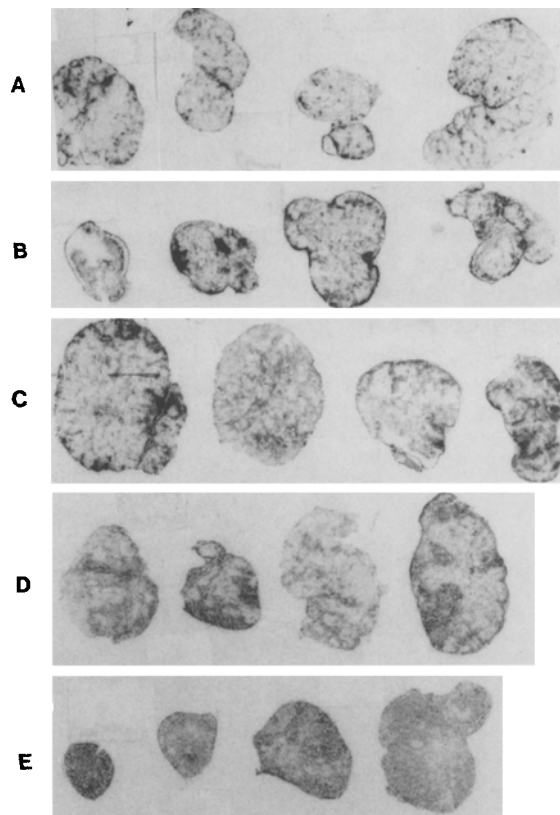
Day 3

Fig. 2. Dose response of NP-4 IgG distribution in GW-39 tumors 3 days after injection of 100 µCi ^{125}I-NP-4 at (**A**) 10 µg (**B**) 100 µg, (**C**) 200 µg, (**D**) 400 µg and (**E**) 800 µg unlabeled antibody

antigen in a small (0.2-g)tumor (Boerman, Sharkey, Blumenthal, Aninipot, and Goldenberg, manuscript in preparation). This is in good agreement with our estimate of total antigen (extractable and non-extractable) based on immunoassay measurements (150–200 µg/g = 30–40 µg in a 0.2-g tumor) and antibody accretion studies (30%–40% injected dose/g; therefore, 2.5–3.3 times more antibody is required than what is actually taken up by the tumor). To saturate antigen in larger tumors of 1.0–1.5 g (i.e., no change in the percentage injected dose per gram), we estimated that a minimum of 450 µg unlabeled antibody would be needed (150 µg/g CEA at 30% injected dose per gram). Figure 2 illustrates that the change in NP-4 antibody distri-

bution resulting from an increased protein dose is a dose-dependent phenomenon. At low protein doses (10 µg, Fig. 2A), the heterogeneity of "hot" regions can be appreciated. Escalating the protein dose to 100 µg (Fig. 2B) does not result in a qualitatively different distribution pattern. Coinjection of 200 µg (Fig. 2C) or 400 µg (Fig. 2D) unlabeled NP-4 enhances the homogeneity of antibody distribution. Further dose escalation to 800 µg unlabeled NP-4 (Fig. 2E) resulted in a greater enhancement of antibody distribution; however, the total grain density was reduced, suggesting an over-saturation of antigen and reduction in specific tumor accretion. Therefore, the selection of an optimal protein dose to increase the homogeneity of antibody distribution must be based on an appreciation of tumor size, total tumor antigen and percentage injected dose per gram of antibody accreted by the tumor. As would be expected, for a given high-protein dose (400 µg-one that is not saturating without reducing total antibody accretion), antibody distribution is enhanced more in smaller tumors than in larger tumors (Fig. 3).

To demonstrate that the changes in antibody penetration seen with 400 µg coadministered unlabeled antibody are the result of saturation of tumor antigen, we evaluated the effect that 400 µg isotype-matched irrelevant antibody AFP-7-31 would have on NP-4 distribution. Figure 4 illustrates that the heterogeneous pattern of NP-4 distribution does not change when 400 µg nonspecific antibody is added to the radioantibody.

In order to obtain a more dynamic picture of radioantibody distribution under low and high penetrating conditions, tumors were evaluated 1, 3, 7, and 14 days after injection of NP-4 IgG. Figure 5 (left panel) shows a clear enhancement of antibody penetration as a result of increasing protein dose as early as 1 day after radioantibody injection. Within 7 days of antibody injection, NP-4 distribution has improved even at a low protein dose (10 µg). However, a further increase in NP-4 penetration is indicated in three out of four tumor samples at 400 µg. By day 14, much of the antibody has cleared from the tumor and the effect of the protein dose is less dramatic. Figure 5 (right panel) evaluates the same dynamics of distribution for the antibody Immu-14, a CEA antibody recognizing the same epitope class as NP-4 [21] but with a 10-fold greater affinity. Fujimori et al. [17] have suggested that an increase in antibody affinity from 1×10^8 M^{-1} (e.g., NP-4) to 1×10^9 M^{-1} (e.g., Immu-14) would further increase the heterogeneity of antibody distribution. Our results indicate a clear difference on days 7 and 14 after injection in Immu-14 distribution at a 10-µg dose compared with NP-4;

large tumors   small tumors
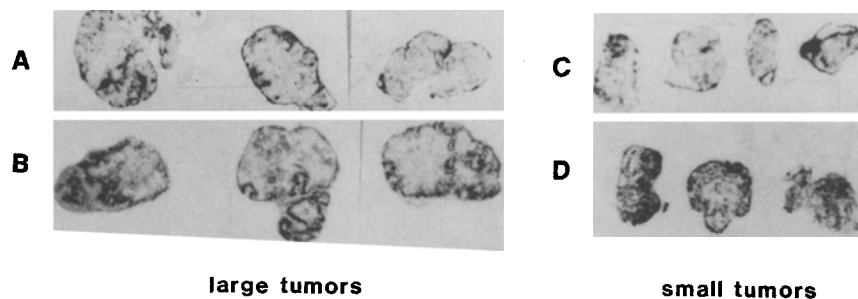
Fig. 3. Effect of protein dose on NP-4 distribution in large (0.8–1.5 g) and small (0.2–0.4 g) tumors 3 days after injection of 100 µCi ^{125}I-NP-4 at 10 µg (**A, C**) or 400 µg antibody (**B, D**)
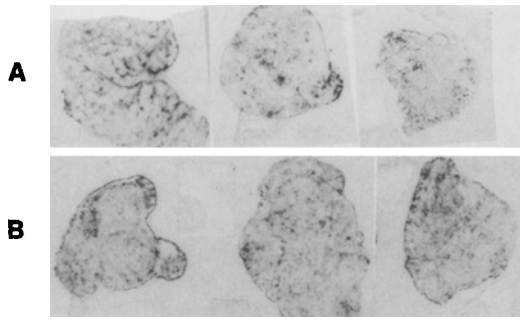
Fig. 4. Effect of a high protein dose (400 μg) of the irrelevant antibody AFP-7-31 on the distribution of 10 μg ^{125}I-NP-4 in GW-39 tumors 3 days after injection: **A** 10 μg ^{125}-NP-4 and **B** 10 μg ^{125}I-NP-4 + 400 μg unlabeled AFP-7-31

Immu-14 retention is increased and its distribution is more heterogeneous. Increasing the protein dose to 400 μg improved Immu-14 distribution at all three evaluation times (3, 7, and 14 days). Even though much of the antibody in the 10-μg dose samples had cleared the tumor by day 14, a much greater amount of antibody remained in the tumor in the 400 μg dose samples, as noted by the intensity of the grain deposition.

Many of the tumor-associated antigens used for antibody-guided therapy are mucins. Therefore, we evaluated the effect of protein dose on the distribution of Mu-9, an antibody directed against CSAp, a mucin antigen. Immunohistochemistry reveals a greater amount of the CSAp antigen in GW-39 tumors (unpublished data). Therefore, a greater amount of antibody would be necessary to saturate the tumor antigen. Figure 6 illustrates the change in distri-

NP-4 IgG   **Immu-14 IgG**
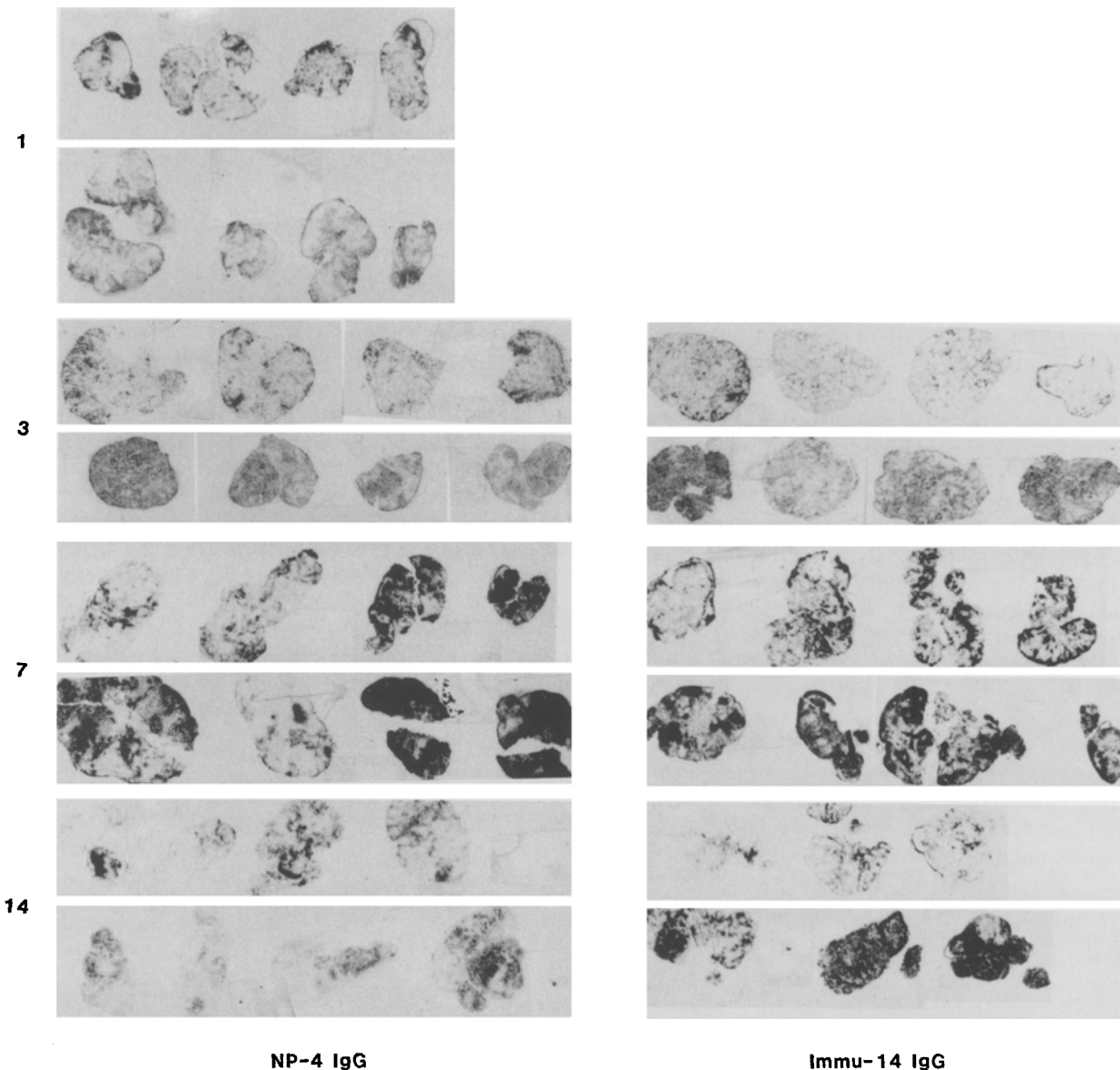
Fig. 5. Effect of protein dose on lower-affinity NP-4 anti-CEA distribution (*left*), and higher-affinity Immu-14 (*right*) anti-CEA distribution as a function of time after injection. Tumors were processed for autoradiography 1, 3, 7, and 14 days after injection of NP-4 and 3, 7, and 14 days after injection of Immu-14. The *upper film strip* in each set was done at 10 μg antibody and the *lower strip* of tumors was done at 400 μg antibody

Mu-9 anti-CSAp

Day 7

Day 14
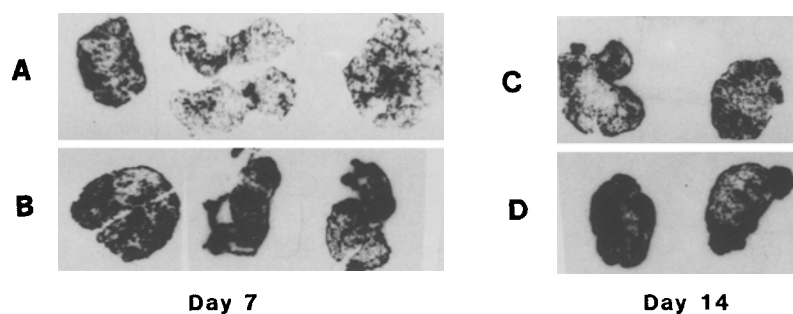
Fig. 6. Protein dose effect in the GW-39 xenograft model for 100 μCi ^{125}I-Mu-9 anti-CSAp at 10 μg (**A, C**) and 800 μg (**B, D**) on days 7 and 14 after injection

GW-39

LS174T

GS-2
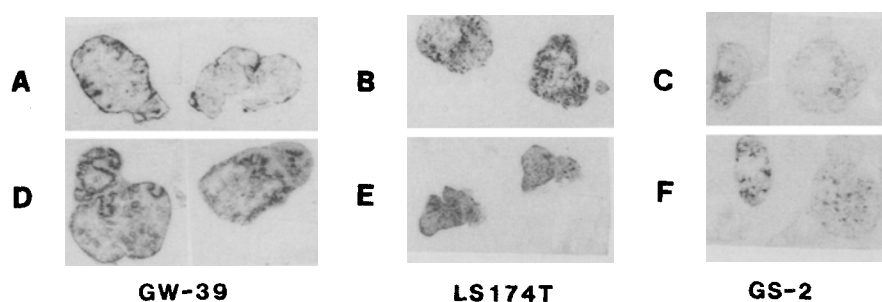
Fig. 7. Comparison of the protein dose effect in three colorectal cancer xenografts: GW-39 signet-ring carcinoma, LS-174T moderately differentiated adenocarcinoma, and GS-2 well-differentiated adenocarcinoma using 100 μCi ^{125}I-NP-4 IgG at 10 μg (**A–C**) and 400 μg (**D–F**)

bution pattern of Mu-9 at 10 μg and 800 μg protein, 7 and 14 days after injection. Mu-9 retention is greater than that of both of the CEA antibodies. Although we did not optimize the high-protein dose concentration, nor did we evaluate earlier times after injection (e.g., 1 and 3 days), one can appreciate a substantial increase in the penetration of Mu-9 at the higher protein dose.

In the last study, we determined whether increasing the protein dose would enhance the distribution of NP-4 anti-CEA in two additional colorectal lines: LS174T, an adenocarcinoma with high antibody accretion, and the GS-2 tumor with low antibody accretion but high antigen content (Blumenthal et al., manuscript in preparation). Figure 7 reveals that the effect of 400 μg on NP-4 distribution seen in GW-39 tumors can also be appreciated in LS174T but not in GS-2. In this study, as in all previous ones, increases in the homogeneity of antibody distribution at a high protein dose are variable from tumor to tumor. Variability in the density of grains can also be appreciated within a single tumor sample, even under these improved conditions. The results presented are all qualitative and can be easily visualized. However, further quantification to determine the coefficient of variation of the density in individual pixels in these tumor samples, taken from low- and high-protein treatments, would be beneficial.

Discussion

The inaccessibility of poorly vascularized regions of solid tumors to a cytotoxic agent such as an antibody conjugate would be expected to influence the efficacy of that agent. There is an increasing recognition that poor penetration of chemotherapeutic drugs into solid tumors may be an im-

portant aspect of cytotoxic drug resistance [26, 31]. Tumor size, growth pattern, and vascularity have been shown to be important physiological factors regulating the penetration of cytotoxic agents.

It has been suggested that nonuniform distribution of radioantibodies in solid tumors is a function of peculiarities found in the tumor microcirculation. Theoretical models have suggested that the relatively high vascular permeability in tumors results in increased endogenous proteins, in the interstitium, causing an elevation in the interstitial osmotic pressure [45]. The elevated interstitial pressure counters the high hydraulic conductivity of tumor vessels, thus lowering fluid extravasation [22, 52]. Once a radiolabeled antibody penetrates the endothelial lining, it is thought that its transport is further retarded by the large interstitial space. The different distribution patterns of the specific and the irrelevant antibodies as early as day 3 in our studies suggest that, in this tumor model, interstitial pressure may not be an important factor regulating antibody penetration.

The vascular barriers that do exist are known to be greatest in larger tumors; as tumors increase in size, the vascular surface area decreases, resulting in a reduction in transvascular exchange and an increase in intercapillary distance, which in turn results in longer times for the radioantibody to reach all areas of the tumor. In addition, as tumors grow, interstitial pressure rises, presumably because of the proliferation of tumor cells in a confined space and the absence of functioning lymphatic vessels [23]. These differences in vascular physiology between small and large tumors represent the rationale for studying mAb distribution in tumors of varying size. Our studies have indicated a more uniform distribution of antibody in smaller tumors than in larger ones at a low protein dose.

According to mathematical models [17, 25, 46], one approach that might be useful to reduce the heterogeneity of antibody distribution is to increase the antibody (protein) dose in order to saturate all antigenic sites and permit the antibody conjugate to bind at random throughout the tumor. We have evaluated antibody penetration following injection of a range of 1–800 µg unlabeled antibody and have found a qualitative enhancement of antibody distribution in large (1-g) tumors at 400–800 µg protein. Several animal studies have demonstrated that the amount of antibody taken up by a tumor is not dependent on the dose of antibody protein administered [1, 41, 50]. However, in our model, 800 µg is an over-saturating dose for this size of tumor, and therefore resulted in a reduction in total antibody accretion, which would effect a reduction in the total radiation dose delivered to the tumor. This observation indicates the importance of titrating the unlabeled antibody dose to maximize antibody penetration and minimize the loss in antibody uptake.

Our results also indicate that even when the total antibody taken up does not change when protein doses are increased (e. g., at 400 µg), its microscopic localization may change, thereby influencing the microdosimetry and therapeutic efficacy of the antibody conjugate (i. e., a scattered distribution of high-dose areas vs a more homogeneous distribution of lower doses). Direct tissue counting alone, as has been done in the past [1, 41, 50], would not provide this information.

The next question that should be addressed is whether the increase in the uniformity of radioantibody distribution within the tumor will result in improved tumor therapy. In one recent study, we demonstrated that NP-4 F(ab′)2 could be equally therapeutic to the intact IgG in GW-39 tumors grown in the hamster cheek pouch, even though the radiation dose delivered by the fragment was less than the dose delivered by the IgG. The intact antibody distribution was restricted to a thin layer of tumor cells at the perimeter of the mass, while the F(ab′)2 fragment distributed through several cell layers [4], an observation that has also been made by others [37, 38]. We postulated that this phenomenon might explain the equivalent tumoricidal effect of the IgG and F(ab′)2 [43]. Studies are in progress to evaluate the therapeutic efficacy of a noncurative dose of a radiolabeled IgG under "normal" (low-protein, non-saturating) conditions, "enhanced penetrating" conditions (saturating), and "enhanced penetration but lower specific uptake" (over-saturating) conditions. The hypothesis in these studies is that improved antibody penetration will result in a greater tumoricidal effect as a result of a more uniform delivery of the radiation dose throughout the tumor. However, other possibilities also exist. Reducing the intense "hot spots" seen in the low-protein tumor autoradiograms might reduce the tumoricidal effect of the radioantibody. We have recently observed a dramatic reduction in tumor vascular activity and a reduction in the number of tumor vessels following a single dose of radioantibody [6]. We suggested that this suppression in tumor vascular function might be a direct result of radioantibody localizing around tumor vessels and delivering a substantial radiation dose in the region of these vessels. If vascular suppression contributes to the tumoricidal effect of radioantibody therapy, then en-

hancing the penetration of radioantibody would reduce the radiation dose delivered around tumor vessels, and thereby reduce the therapeutic effect.

Another possibility might exist that would prevent a more uniform distribution of antibody from resulting in enhanced therapeutic efficacy. The heterogeneity in tumor microcirculation and resulting ischemia subsequent to physical compression of vessels [24, 48] may result in hypoxia and zones of necrosis within tumors. This state of hypoxia within the tumor results in resistance to chemo- and radiotherapy and will therefore also limit the therapeutic efficacy of radiolabeled antibodies [47]. In addition, low tumor oxygen tension has been reported to reduce expression of two melanoma-associated antigens on the human FME melanoma, independent of cell cycle [10]. If the oxygen microenvironment negatively affects the antigenic properties of cancer cells, it may complicate the use of cytotoxic agents conjugated to tumor-localizing antibodies. Thus, improving the penetration of antibodies may result in more of the antibody being distributed to hypoxic tumor regions. However, one report has demonstrated that regional hypoxia may be short-lived; i. e., vessels are compressed and then relax again such that hypoxia measured at one location may not be there minutes later [33]. The use of radiolabeled antibodies may overcome the limitation imposed by short-term hypoxia because of the time required for maximal accretion and the duration of radioantibody retention within the tumor. These issues require further investigation.

Another factor that has been suggested to affect tumor targeting and antibody distribution is antibody affinity. One report claims that a high-affinity antibody is preferable because of the longer retention of antibody [28]. Another study claims that a low-affinity antibody is advantageous because it would result in more uniform distribution [29]. In general, antibody affinity for tumor targeting is in the range of $10^8–10^{12}M^{-1}$ [43]. Thomas et al. have developed a mathematical model to determine how antibody affinity affects tumor uptake. The model predicts that as antibody affinity increased from 10^8 to $10^{13}M^{-1}$, specific antibody uptake would increase over 100-fold, but only if the protein dose was increase 100-fold from 0.6 nM (typical scanning dose) to 60 nM [46]. The validity of this model is supported by reported values [11]. We recently reported a small improvement in antibody accretion when Immu-14 anti-CEA ($1 \times 10^9M^{-1}$), an antibody with 10-fold higher affinity than NP-4 anti-CEA [11, 21] and recognizing the same class epitope on CEA [21, 30], is used. mAb accretion appears to be more responsive to changes in affinity in larger tumors (>0.6 g) than in smaller tumors (<0.2 g). With respect to antibody distribution, mathematical models suggest that a single log difference in affinity can produce significant differences in antibody distribution [17]. Our results indicate that we observe better retention of the higher-affinity Immu-14, and that regional distribution of Immu-14 is more heterogeneous than that of lower-affinity NP-4 7 and 14 days after injection.

We have demonstrated differences in the magnitude of radioantibody uptake by the GW-39 tumor grown in several sites [3] and by the GW-39, LS174T, and GS-2 tumors grown in the same subcutaneous site of the nude mouse [5].

Several physiological factors, including total vascular activity, tumor and serum antigen content, and antigen accessibility have been shown to differ between these models (R. Blumenthal et al., manuscript in preparation). Of particular interest is the observation that a structural barrier exists in the GS-2 tumor model, which results in antibody distribution to the basolateral surface of glands where it cannot bind to the antigen, which is located within gland cells and on the apical surface of glands. The structural barrier that exists in the GS-2 tumor, which appears to be similar to that seen in the HRA-19 adenocarcinoma line [39], cannot be overcome by increasing the protein dose.

The results presented here highlight the importance of evaluating theoretical concepts in established experimental models. The physiological principles established from this research are applicable not only to radioimmunoconjugates, but to drug- and toxin-antibody conjugates and to therapy with other anticancer agents, such as cytokines, growth inhibitors, and biological response modifiers.

References

1. Badger CC, Krohn KA, Peterson AV, Shulman H, Bensh IP (1985) Experimental radiotherapy of murine lymphoma with ^{131}I-labeled Anti-Thy 1.1 monoclonal antibody. Cancer Res 45: 1536
2. Blumenthal RD, Sharkey RM, Kashi R, Goldenberg DM (1989) Comparison of the therapeutic efficacy and host toxicity of two different ^{131}I-labeled antibodies and their fragments in the GW-39 colonic cancer xenograft model. Int. J Cancer 44: 292
3. Blumenthal RD, Sharkey RM, Kashi R, Natale AM, Goldenberg DM (1989) Influence of animal host and tumor implantation site on radioantibody uptake in the GW-39 human colonic cancer xenograft. Int J Cancer 44: 1041
4. Blumenthal, RD, Sharkey RM, Goldenberg DM (1990) Current perspectives and challenges in the use of monoclonal antibodies as imaging and therapeutic agents. Adv Drug Deliv Rev 4: 279
5. Blumenthal RD, Sharkey RM, Kashi R, Natale AM, Goldenberg DM (1990) Physiological parameters responsible for difference in radioantibody uptake in experimental human tumor models (abstract). Proc Am Assoc Cancer Res 31: 61
6. Blumenthal RD, Sharkey RM, Kashi R, Goldenberg DM (1991) Suppression of tumor vascular function following radioimmunotherapy: Implications for multiple cycle treatments. Selec Cancer Ther (in press)
7. Bosslet K, Keweloh HCH, Hermentin P, Muhrer KH, Schultz G (1990) Percolation and binding of monoclonal antibody BW494 to pancreatic carcinoma tissues during high dose immunotherapy and consequences for future therapy modalities. Br J Cancer 62 (Suppl 10): 37
8. Buchegger F, Vacca A, Carrel S, Schreyer M, Mach JP (1988) Radioimmunotherapy of human colon carcinoma by ^{131}I-labeled monoclonal anti-CEA antibodies in a nude mouse model. Int J Cancer 41: 127
9. Carrasquillo JA, Krohn KA, Beumier P, McGriffin RW, Brown JP, Hellstrom KE, Hellstrom I, Larson SM (1984) Diagnosis and therapy for solid tumors with radiolabeled antibodies and immune fragments. Cancer Treat Rep 68: 317
10. Davies CL, Petterson EO, Lindmo T (1989) Change in antigen expression in human FME melanoma cells after exposure to hypoxia and acidic pH, alone or in combination. Int J Cancer 43: 350
11. Dykes PW, Bradwell AR, Chapman CE, Vaughan ATM (1987) Radioimmunotherapy of cancer: clinical studies and limiting factors. Cancer Treat Rev 14: 87
12. Esteban JM, Schlom J, Morrex F, Colcher D (1987) Radioimmunotherapy of athymic mice bearing human colon carcinomas with monoclonal antibody B72.3: histological and autoradiographic study of the effect on tumor and normal organs. Eur J Cancer Clin Oncol 23: 643
13. Ettinger DS, Order SE, Wharman MD, Parker MK, Klein JL, Leichner K (1982) Phase I–II study of isotopic immunoglobulin therapy for primary liver cancer. Cancer Treat Rep 66: 289
14. Fand I, Sharkey RM, McNally A, Brill AB, Som P, Yamamoto F, Primus FJ, Goldenberg DM (1986) Quantitative whole-body autoradiography of radiolabeled antibody distribution in a xenografted human cancer model. Cancer Res 46: 271
15. Fand I, Sharkey RM, Primus FJ, Cohen SA, Goldenberg DM (1987) Relationship of radioantibody localization and cell viability in a xenografted human cancer model as measured by whole-body autoradiography. Cancer Res 47: 2177
16. Fawwaz RA, Wang TST, Srivastava SC, Hardy MA (1986) The use of radionuclides for tumor therapy. Nucl Med Biol 13: 429
17. Fujimori K, Covell DG, Fletcher JE, Weinstein JN (1990) A modeling analysis of monoclonal antibody percolation through tumors: a binding-site barrier. J Nucl Med 31: 1191
18. Gold DV, Nocera MA, Stephens R, Goldenberg DM (1990) Murine monoclonal antibodies to colon specific antigen-p. Cancer Res 50: 6405
19. Goldenberg DM, Witte S, Elster K (1966) GW-39: a new human tumor serially transplantable in the golden hamster. Transplantation 4: 760
20. Goldenberg DM, Gaffar SA, Bennett SJ, Beach JL (1981) Experimental radioimmunotherapy of a xenografted human colonic tumor (GW-39) producing carcinoembryonic antigen. Cancer Res 41: 4354
21. Hansen HJ, Nemann ES, Ostello F, Moskie LA, Sharkey RM, Goldenberg DM (1989) Preclinical comparison of two specific anti-carcinoembryonic antigen (CEA) MAbs, NP-4 and Immu-14, in athymic nude mice bearing GW-39 human colon carcinoma xenografts (abstract). Proc Am Assoc Cancer Res 30: 414
22. Jain RK (1987) Transport of molecules across tumor vasculature. Cancer Metastasis Rev 6: 559
23. Jain RK (1987) Transport of molecules in the tumor interstitium: a review. Cancer Res 47: 3039
24. Jain RK (1988) Determinants of tumor blood flow: a review. Cancer Res 48: 2641
25. Jain RK, Baxter LT (1988) Mechanism of heterogeneous distribution of monoclonal antibodies and other macromolecules in tumors: significance of elevated interstitial pressure. Cancer Res 48: 7022
26. Kerr DJ, Kaye SB (1987) Aspects of cytotoxic drug penetration, with particular references to anthracyclines. Cancer Chemother Pharmacol 19: 1
27. Kerr DJ, Wheldon TE, Hydns S, Kaye SB (1988) Aspects of cytotoxic drug penetration with particular reference to anthracyclines. Xenobiotica 18: 641
28. Mach JP, Buchegger F, Forni M, Ritschard J, Berche C, Lumbroso JD, Schreyer M, Giardet C, Accolla RS, Carrel S (1981) Use of radiolabeled monoclonal anti-CEA antibodies for the detection of human carcinomas by external photoscanning and tomoscintigraphy. Immunol Today 2: 239
29. Mason DW, Williams AF (1987) In: Bonavida B, Collier RJ (eds) Membrane mediated cytotoxicity. Liss New York, p 279
30. McConahey PJ, Dixon FJ (1966) A method of trace iodination of proteins for immunologic studies. Int Arch Allergy 29: 185
31. Mattson J, Peterson P (1981) Influence of vasoactive drugs on tumor blood flow. Anticancer Res 1: 59
32. Matzku S, Tilgen W, Kalthoff H, Schmiegel WH, Brocker EB (1988) Dynamics of antibody transport and internalization. Int J Cancer 2 (Suppl) 11
33. Minchinton AI, Durand RE, Chaplin DJ (1990) Intermittant blood flow in the KHT sarcoma-flow cytometry studies using Hoechst 33342. Br J Cancer 62: 195
34. Nederman T, Carlsson J, Malmqvist M (1981) Penetration of substances into tumor tissue – a methodological study on cellular spheroids. In Vitro 17: 290

35. Nederman T, Carlsson J, Kuoppa K (1988) Penetration of substances into tumor tissue. Model studies using saccharides, thymidine and thymidine-5'-triphosphate in cellular spheroids. Cancer Chemother Pharmacol 22: 21

36. Ong GL, Mattes MJ (1989) Penetration and binding of antibodies in experimental human solid tumors grown in mice. Cancer Res 49: 4264

37. Pervez S, Epenetos AA, Mooi WJ, Evans DJ, Rowlinson G, Dhokia B, Krausz T (1988) Localization of monoclonal antibody AUA1 and its $F(ab')_2$ fragments in human tumor xenografts. An autoradiographic and immunohistochemical study. Int J Cancer (Suppl 3): 23

38. Pervez S, Paganelli G, Epenetos AA, Mooi WJ, Evans DJ, Krausz T (1988) Localization of biotinylated monoclonal antibody in nude mice bearing subcutaneous and intraperitoneal human tumor xenografts. Int J Cancer 43 (Suppl 3): 30

39. Pervez S, Kirkland SC, Epenetos AA, Mooi WJ, Evans DJ, Krausz T (1989) Effect of polarity and differentiation on antibody localization in multicellular tumor spheroid and xenograft models and its potential importance for in vivo immunotargeting. Int J Cancer 44: 940

40. Sharkey RM, Filion D, Fand I, Primus FJ, Goldenberg DM (1986) A human colon cancer metastasis model for radioimmunodetection. Cancer Res 46: 3677

41. Sharkey RM, Primus FJ, Goldenberg DM (1987) Antibody protein dose and radioimmunodetection of GW-39 human colon tumor xenografts. Int J Cancer 39: 611

42. Sharkey RM, Pykett MJ, Siegel JA, Alger EA, Primus FJ, Goldenberg DM (1987) Radioimmunotherapy of the GW-39 human colonic tumor xenograft with ^{131}I-labeled murine monoclonal antibody to carcinoembryonic antigen. Cancer Res 47: 5672

43. Sharkey RM, Primus FJ, Shochat D, Goldenberg DM (1988) Comparison of tumor targeting of mouse monoclonal and goat polyclonal antibodies to carcinoembryonic antigen in the GW-39 human tumorhamster host model. Cancer Res 48: 1823

44. Sutherland R, Buchegger F, Schreyer M, Vacca A, Mach JP (1987) Penetration and binding of radiolabeled anti-carcinoembryonic antigen monoclonal antibodies and their antigen binding fragments in human colon multicellular tumor spheroids. Cancer Res 47: 1627

45. Sylven B, Bois I (1960) Protein content and enzymatic assays of interstitial fluid from some normal tissues and transplanted mouse tumors. Cancer Res 20: 831

46. Thomas GD, Chappell MJ, Dykes PW, Ramsden DB, Godfrey KR, Ellis JRM, Bradwell AR (1989) Effect of dose, molecular size, and protein binding on tumor uptake of antibody or ligand: a biomathematical model. Cancer Res 49: 3290

47. Trotter MJ, Chaplin DJ, Olive PL (1989) Use of carbocyanate dye as a marker of functional vasculature in murine tumors. Br J Cancer 59: 706

48. Vaupel P, Fortmeyer HP, Runkel S, Kallinowski F (1987) Blood flow, oxygen consumption and tissue oxygenation of human breast cancer xenografts in nude rats. Cancer Res 47: 3496

49. Vessella RL, Alvarez V, Chiou RK, Rodwell J, Elson M, Palme D, Shafer R, Lange P (1987) Radioimmunoscintigraphy and radioimmunotherapy of renal cell carcinoma xenografts. NCI Monogr 3: 159

50. Wahl RL, Liebert M, Wilson BS (1986) The influence of monoclonal antibody dose on tumor uptake of radiolabeled antibody. Cancer Drug Deliv 3: 243

51. West GW, Weichselbaum R, Little JB (1980) Limited penetration of methotrexate into human osteosarcoma spheroids as a proposed model for solid tumor resistance to adjuvant chemotherapy. Cancer Res 40: 3665

52. Wiig H, Tveit E, Hultborn R (1982) Interstitial fluid pressure in DMBA-induced rat mammary tumors. Scand J Clin Lab Invest 42: 159

53. Zalcberg JR, Thompson CH, Lichtenstein M, McKenzie IFC (1984) Tumor immunotherapy in the mouse with the use of ^{131}I-labeled monoclonal antibodies. J Natl Cancer Inst 72: 697